South East Asian J. of Mathematics and Mathematical Sciences
Vol. 16, No. 3 (2020), pp. 295-310

ISSN (Online): 2582-0850

ISSN (Print): 0972-7752

A NUMERICAL INVESTIGATION OF CHEMICALLY REACTING 2D WILLIAMSON FLUID OVER A VERTICAL EXPONENTIALLY STRETCHING SURFACE

K. S. Srinivasa Babu, A. Parandhama* and R. Bhuvana Vijaya

Department of Mathematics,
J N T U A College of Engineering,
Ananthapuramu, Andhra Pradesh - 515002, INDIA
E-mail : ssbkasibhotla@gmail.com

*Department of Mathematics,
Sree Vidyanikethan Engineering College,
Tirupati, Andhra Pradesh - 517102, INDIA

(**Received:** *Sep. 04, 2020* **Accepted:** *Oct. 17, 2020* **Published:** *Dec. 30, 2020*)

Abstract: This article presents a novel modeling corresponding to a mixed convective magnetohydrodynamic chemically reacting two-dimensional Williamson fluid (a non-Newtonian fluid) through a vertical exponentially stretchable impermeable surface followed by temperature and concentration distributions. Temperature, concentration, stretching velocity and applied magnetic field are treated as functions with exponential variation. Equations which are governing the flow and both transfer rates (heat & mass) are transferred into ODEs and solved them by means of a shooting technique along with RK-4th order method. Responses of dimensionless quantities (fluid velocity, temperature and concentration) including with friction coefficient, both transfer rates (heat and mass) corresponding to different parameters are illustrated by means of plots and tables. From this study, we found that the increased Williamson parameter and magnetic effect lowers the fluid velocity. Increased magnetic effect and thermal biot number elevates the temperature. Furthermore, concentration boundary layer is observed to be thicker by concentration biot number and thinner by chemical reaction parameter.

Keywords and Phrases: MHD, Mixed convection, Williamson fluid, Exponential stretching, Chemical reaction.

2010 Mathematics Subject Classification: 76W05, 76E06, 76A05, 80A32.

1. Introduction

From the last two decades there is noticeable significance on non-Newtonian fluids because of their enormous applications in industries, engineering fields and production fields also. Coal-oil slurries, shampoo, paints, clay coating and suspensions, grease, cosmetic products, custard, physiological liquids such as blood, bile, synovial fluids comes under this category. The simulation of such fluids and their characteristics is a challenging area to the researchers. It is difficult to simulate the critical characteristics of such fluids by using Navier-Stokes equations. To identify a relation between shear stress and rate of strain in non-Newtonian fluids versus viscous fluids is very complicated task. The visco-elastic characteristics in such fluids will have more complexity in the obtained equations on comparison with Navier-Stokes equations. In 1929, Williamson [28] considered the flow of pseudo plastic materials and proposed a modeling with the equations to depict the pseudo plastic fluid flows and their behavior explained with an experimental verification. Williamson fluid is a pseudo plastic fluid and it belongs to non-Newtonian fluid category. In recent years, appreciable investigations have been done by several researchers on this fluid. Valid conclusions have been traced out by several authors in their research works using different geometries.

The examination of two-dimensional flow over stretching surfaces is another important aspect of industrial as well as engineering applications. Paper production, hot rolling, metal spinning, spinning of fibers, glass blowing, drawing plastic films etc are examples of such application areas. The rate of change in temperature via stretching surfaces is the reason for the quality of the final output. Stretching surfaces may be linear or non-linear, slandering, exponential, quadratic variations in velocity as well as temperature fields. Magyari and Keller [17], Elbahbeshy [8] discussed the behavior and the characteristics of heat transfer along the exponentially stretching surfaces. Partha et al. [22] concentrated on a mixed convective flow and heat transfer characteristics via exponentially stretched surface in addition to viscous dissipation. They have obtained similarity solutions from which they reported the significant influence of viscous dissipation and buoyancy effects on flow and heat transfer. Tsai et al. [27] focused on the flow as well as heat transfer by using Chebyshev finite difference method with non-uniform heat source over an unsteady stretching horizontal sheet. A numerical approach that gives the magnetic field effects on thermal boundary layer over an exponentially stretching continuous surface by Al-Odat et al. [1]. A similar investigation is discussed by Dulal Pal

[20] which describes the mixed convective heat transfer through the exponential stretching surface in the boundary layers with magnetic field. Khalili et al. [19] studied the magnetohydrodynamic boundary layer flow and heat transfer behaviors over an exponentially stretching sheet with chemical reaction, radiation and heat sink. Isa et al. [23] team presented a similar study of magnetohydrodynamic mixed convective flow and the transfer of heat using exponential temperature variation past exponentially stretching sheet. Based on the above research works, a similar investigation carried out by Srinivasa Babu et al. [25] in which they reported the magnetohydrodynamic mixed convective flow and behavior of heat transfer along exponentially stretchable vertical sheet. Jayachandra Babu and Sandeep [10] investigated the cross-diffusion effects of MHD non-Newtonian fluid flow over a stretching slandering sheet. Anuar Ishak et al. [6] also discussed numerically the phenomenon of heat transfer over an unsteady stretching surface. A similar investigation found for three-dimensional flow and transfer rate of heat over an exponentially stretched surface by Liu et al. [16]. Mukhopadhyay et al [18] discussed free convective boundary layer flow and heat transfer along a permeable stretching surface with additional impact of thermal radiation and viscosity variations. Nadeem et al. [24] presented the thermal radiation effects on the boundary layer flow of a Jeffrey fluid from an exponentially stretched sheet. By considering an inclined permeable stretching sheet along with the effects of non-linear radiation and internal heat source, the behavior of flow and heat transfer for a magnetohydrodynamic fluid has been worked out by Amit Parmar [21]. A mathematical analysis has been reported by Ganesh Kumar et al. [9] in which they have presented the two-phase boundary layer flow and heat transfer mechanism of a Williamson liquid along with fluid particle suspension and non-linear thermal radiation effects over a stretched sheet. Using a finite difference technique, Bilal et al. [7] discussed and presented numerical results of Williamson fluid flow past a cylindrical surface with a support of thermal stratification. Numerical works have been published on micropolar fluids with different geometries and with various physical effects which are mentioned in [3, 4, 12, 13, 14, 15]. Kumar et al. [5] studied numerically the MHD Cattaneo-Christov flow over a cone and a wedge under variable heat source/sink. Tlili et al. [26] discussed the stream and energy transport in MHD dissipative ferro and hybrid ferrofluids under uneven heat rise/fall along with radiation effects. They reported the simultaneous solutions for both ferro and hybrid ferrofluid cases. Recently, Kumar et al. [2] reported the flow and heat transfer characteristics of Casson fluid from an exponentially stretching curved surface under thermal radiation and convective boundary conditions. Kumar et al. [11] deliberated the convective heat transfer phenomenon in MHD micropolar fluid via

an exponentially stretching curved surface near stagnation point along with thermal radiation, non-uniform heat source/sink, Joule heating and variable thermal conductivity.

Motivation from the above researchers and based on the available literature, we studied numerically, the mixed convective MHD 2D Williamson fluid via exponentially vertical stretching surface with appropriate conditions, both transfer rates (heat and mass). Here R-K 4^{th} order based on shooting technique is used to solve the resultant equations. We considered applied convective boundary conditions, exponential applied magnetic field $B(x) = B_0 e^{x/2L}$, Viscous dissipation, buoyancy force taken into consideration. The results are discussed through plots and tables.

2. Problem formulation

Here we considered the incompressible and electrically conducting steady two-dimensional flow of Williamson fluid along an exponentially vertical stretching surface with exponential temperature and concentration distributions, subjected to a transverse magnetic field is considered. x-axis is along the direction of the surface and y-axis is taken to be perpendicular to sheet.
The stress tensor involved in Williamson model is given by [28]

$$S = -pI + \tau \tag{i}$$

$$\tau = \left[\mu_\infty + \frac{\mu_0 - \mu_\infty}{1 - \Gamma\dot{\gamma}}\right]\dot{\gamma} \tag{ii}$$

Where p means the pressure, I means Identity vector, τ means extra stress tensor, μ_0 and μ_∞ are the viscosity at zero shear rate and at infinity, Γ denotes the time constant.
We consider the equation (ii), the case for which $\mu_\infty = 0$ and $\Gamma\dot{\gamma} < 1$ and $\dot{\gamma}$ can be derived as

$$\dot{\gamma} = \sqrt{\frac{1}{2}\sum_i\sum_j \dot{\gamma_{ij}}\dot{\gamma_{ji}}} = \sqrt{\frac{1}{2}\prod} \tag{iii}$$

Here $\prod$ taken as second invariant strain tensor.
So, equation (ii) becomes

$$\tau = \left[\frac{\mu_0}{1 - \Gamma\dot{\gamma}}\right]\dot{\gamma} \quad \text{or} \quad \tau = \mu_0[1 + \Gamma\dot{\gamma}]\dot{\gamma} \quad \text{(based on binomial expansion)} \tag{iv}$$

The governing equations of this modeling are presented below :

$$\frac{\partial u}{\partial x} + \frac{\partial v}{\partial y} = 0 \tag{1}$$

$$u\frac{\partial u}{\partial x}+v\frac{\partial u}{\partial y}=\nu\frac{\partial^2 u}{\partial y^2}+\sqrt{2}\Gamma\left(\frac{\partial u}{\partial y}\right)\frac{\partial^2 u}{\partial y^2}+g\beta_T(T-T_\infty)+g\beta_C(C-C_\infty)-\frac{\sigma B^2(x)}{\rho}u \quad (2)$$

$$u\frac{\partial T}{\partial x}+v\frac{\partial T}{\partial y}=\frac{k}{\rho c_p}\frac{\partial^2 T}{\partial y^2}+\frac{\sigma B^2(x)}{\rho c_p}u^2+\frac{\nu}{c_p}\left(\frac{\partial u}{\partial y}\right)^2 \quad (3)$$

$$u\frac{\partial C}{\partial x}+v\frac{\partial C}{\partial y}=D_m\frac{\partial^2 C}{\partial y^2}-k_0(C-C_\infty) \quad (4)$$

Where u and v are taken as components of velocity in the directions of x and y respectively. $T-$ the temperature, $C-$ the concentration, $g-$ the acceleration due to gravity, $\rho-$ the density, $\mu-$ the viscosity coefficient, $\nu-$ the kinematic viscosity, Γ is a positive time constant, β_T, β_C are the coefficients of thermal as well as concentration expansions, $\alpha-$ the thermal diffusivity, D_m- the diffusivity of the medium, c_p- specific heat capacity, k_0- the reaction rate constant.

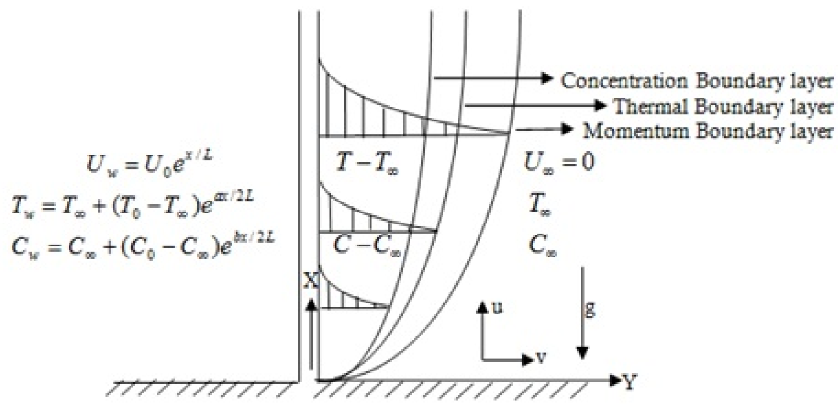

Figure -1: Flow pattern along the surface

Following are the boundary conditions of the present study:

$$u=U_w(x)=U_0e^{x/L},\quad v=0,\quad T=T_w(x),\quad C=C_w(x),\quad -k\frac{\partial T}{\partial y}=h_1(T_0-T),$$

$$-D_m\frac{\partial C}{\partial y}=h_2(C_0-C)\ \text{ at y=0},\quad u=0,\ T\to T_\infty,\ C\to C_\infty\ \text{ as } y\to\infty \quad (5)$$

Here h_1, h_2 indicates coefficients of convective heat and mass transfer respectively and 'k' is thermal conductivity. $T_w(x)=T_\infty+(T_0-T_\infty)e^{ax/2L}$; $C_w(x)=C_\infty+(C_0-C_\infty)e^{bx/2L}$ are the temperature and concentration distributions respectively.

The similarity variables are

$$\eta = y\sqrt{\frac{U_0}{2L\nu}}e^{x/2L}, \psi(x,y) = \sqrt{2LU_0\nu}e^{x/2L}f(\eta),$$
$$T(x,y) = T_\infty + (T_0 - T_\infty)e^{ax/2L}\theta(\eta), \quad C(x,y) = C_\infty + (C_0 - C_\infty)e^{bx/2L}\phi(\eta) \quad (6)$$

The stream function ψ is introduced through $u = \frac{\partial\psi}{\partial y}$ and $v = -\frac{\partial\psi}{\partial x}$. Also, a, b are similarity variables corresponding to temperature and concentration respectively and treated them as parameters of the temperature distribution and concentration distribution along the surface.
Using similarity variables (6), the equations (2)-(4) becomes

$$f'''(1+\Lambda f'') + ff'' - 2(f')^2 + 2\lambda e^{-2X}\left(\theta e^{\frac{aX}{2}} + N\phi e^{\frac{bX}{2}}\right) - 2Mf' = 0 \quad (7)$$

$$\theta'' + Pr(f\theta' - af'\theta) + Ec.Pr.e^{2X-\frac{aX}{2}}[2M(f')^2 + (f'')^2] = 0 \quad (8)$$

$$\phi'' + Sc(f\phi' - bf'\phi) - Sc.K_r.e^{-X}\phi = 0 \quad (9)$$

and the conditions will be

$$f = 0, f' = 1, \theta = \left(\frac{1}{Bi_T}\right)\theta' + e^{-\frac{aX}{2}}, \phi = \left(\frac{1}{Bi_C}\right)\phi' + e^{-\frac{bX}{2}} \quad \text{at} \quad \eta = 0$$
$$f' \to 0, \theta \to 0, \phi \to 0, \quad \text{as} \quad \eta \to \infty \quad (10)$$

Here $X = x/L$ is the non-dimensional coordinate; $Bi_T = \frac{h_1 y}{\eta k}$, $Bi_C = \frac{h_2 y}{\eta k}$ are the Biot numbers (thermal and concentration); $\Lambda = \Gamma\sqrt{\frac{U_0^3 e^{3X}}{\nu L}}$ is the Williamson parameter; $Gr = \frac{g\beta_T(T_0-T_\infty)L^3}{\nu^2}$ is the thermal Grashof number and; $Re = \frac{U_0 L}{\nu}$ is the Reynolds number; $\lambda = \frac{Gr}{Re^2}$ is the mixed convection parameter; $N = \frac{\beta_C(C_0-C_\infty)}{\beta_T(T_0-T_\infty)}$ is the buoyancy ratio; $Pr = \nu/\alpha$ is the Prandtl number; $Ec = \frac{U_0^2}{c_p(T_0-T_\infty)}$ is the Eckert number; $Sc = \frac{\nu}{D_m}$ is the Schmidt number; $K_r = \frac{2Lk_0}{U_0}$ is the Chemical reaction parameter; $M = \frac{Ha^2}{Re} = \frac{\sigma B_0^2 L}{\rho U_0}$ is magnetic field parameter.
The local skin friction is termed as $\tau_w = \mu\left[\frac{\partial u}{\partial y} + \frac{\Gamma}{\sqrt{2}}\left(\frac{\partial u}{\partial y}\right)\right]_{y=0}$ and the dimensionless friction coefficient is $\frac{C_{fx}}{(Re_x/2)^{-0.5}} = f''(0) + \frac{\Lambda}{2}(f''(0))^2$, where $C_{fx} = \frac{\tau_w}{\rho U_w^2}$, $Re_x = \frac{xU_w(x)}{\nu}$ (local Reynold's number). Local Nusselt number, Nu_x is given by $Nu_x = \frac{xq_w}{k(T_0-T_\infty)}$ and the dimensionless heat transfer coefficient is $\frac{Nu_x}{\sqrt{X/2}\sqrt{Re_X}} = \theta'(0)$, where $q_w = -k\left(\frac{\partial T}{\partial y}\right)_{y=0}$ is the heat flux at the wall.

Also, local Sherwood number, Sh_x is given by $Sh_x = \frac{xq_m}{D_m(C_0 - C_\infty)}$ and the dimensionless mass transfer coefficient is $\frac{Sh_x}{\sqrt{X/2}\sqrt{Re_x}} = -\phi'(0)$, where $q_m = -D_m\left(\frac{\partial C}{\partial y}\right)_{y=0}$ is the mass flux at the wall.

3. Numerical Procedure

The non-linear ODEs from (7) to (9) including boundary conditions (10) solved by make use of shooting method based on Runge – Kutta method in MATLAB. For this, we have rewritten the equations (7), (8) and (9) into a set of seven simultaneous ODEs as shown :

Let $f_1 = f$, $f_2 = f'$, $f_3 = f''$, $f_4 = \theta$, $f_5 = \theta'$, $f_6 = \phi$ and $f_7 = \phi'$. (Here the prime means derivative with respect to η). Thus $f_1' = f_2$, $f_2' = f_3$,

$$f_3' = \frac{1}{(1+\Lambda f'')}\left[2(f')^2 - ff'' - 2\lambda e^{-2X}\left(\theta e^{\frac{aX}{2}} + N\phi e^{\frac{bX}{2}}\right) + 2Mf'\right],$$

$f_4' = f_5$,

$$f_5' = Pr(af'\theta - f\theta') - Ec.Pr.e^{2X - \frac{aX}{2}}[2M(f')^2 + (f'')^2],$$

$f_6' = f_7$,

$$f_7' = Sc(bf'\phi - f\phi') + Sc.K_r.e^{-X}\phi.$$

For the responses of the system, we employed a shooting technique depending on RK 4^{th} order method. For one set of values of the parameters, values of $f''(0)$, $\theta'(0)$ and $\phi'(0)$ are assumed and the system of first order ordinary differential equations is solved as an initial value problem from $\eta = 0$ to $\eta = \eta_\infty$ (η_∞ is a large value of η) using RK method. The values of f', θ and ϕ at η_∞ are compared with their expected values and accordingly $f''(0)$, $\theta'(0)$ and $\phi'(0)$ are modified and the system of equations again solved as an initial value problem. The procedure is repeated a number of times till the values of f', θ and ϕ at η_∞ are very close to the expected values. By the above mentioned procedure we can get values of $f''(0)$, $\theta'(0)$ and $\phi'(0)$ for one set of values of the parameters of the study. Similarly we determined the values of $f''(0)$, $\theta'(0)$ and $\phi'(0)$ for all possible values of the parameters of the study. Using the initial conditions, the equations are solved to get the velocity, temperature and concentration distributions and also the quantities like skin friction, heat and mass transfer rates. During this process, the step size and convergence criteria are maintained as 0.001 and 10^{-6} in all cases.

4. Results and Discussion

Using a numerical method, the responses are observed for velocity of the fluid, temperature distribution and concentration distribution for certain values of physical parameters given as M, a, b, Λ, Ec, Pr, λ, N, Sc, K_r, Bi_T, Bi_C and X

which are included in the equations (7)–(9). The results obtained for a particular selection of values given to the parameters utilized in the problem. The impacts of velocity profile, both transfer rates (heat and mass) are presented through plots. The calculated values of skin friction, Nusselt number and Sherwood number are mentioned in Table-2 for distinct values of the important parameters of present investigation.

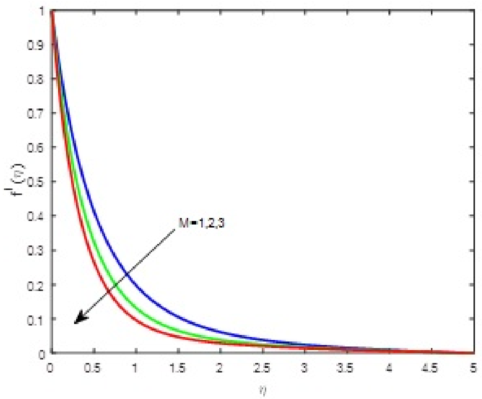

Fig. 2 Consequence of M on Velocity

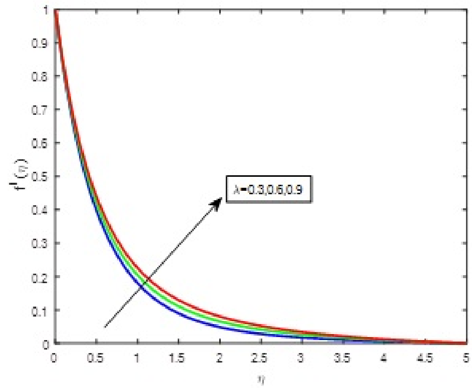

Fig. 3 Consequence of λ on Velocity

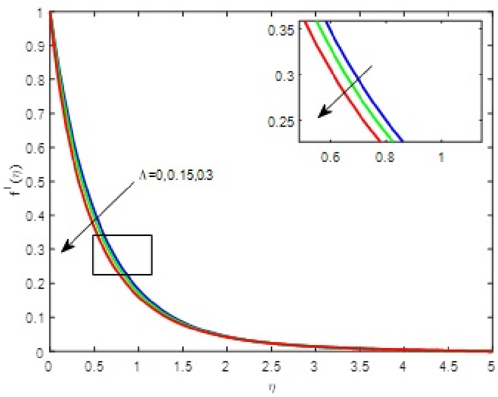

Fig. 4 Consequence of Λ on Velocity

Variations in fluid velocity with different physical parameters are presented in figures 2 to 4. In Fig. 2, Fluid velocity is observed to be diminished with enhancement in magnetic parameter (M). The reason behind it is the increased magnetic effect leads to an enhancement of Lorentz forces and hence the magnitude of the velocity is reduced. From fig. 3, it was identified that the dimensionless fluid velocity rises when increasing mixed convection parameter (λ) due to the buoyancy effect. From fig. 4, it was found that fluid velocity slightly diminished with a rise in Williamson parameter (Λ). By the increment in Λ, the fluid gets some resistance to flow, so that the momentum boundary layer becomes thinner. We observed that there is no much more variation in momentum boundary layer thickness for the parameters M, Λ and λ.

The responses of temperature of the fluid $\theta(\eta)$ are shown in the figures 5 to 8. Fig. 5 gives us the Eckert number (Ec) impact on temperature field. As Eckert number is the ratio of advective transport to heat dissipation, internal heat will be produced so that the temperature profiles are enhanced. From fig. 6, one can see that whenever mixed convection parameter (λ) takes larger values, the temperature becomes down. The impact of thermal biot number (Bi_T) verses temperature field was presented in fig. 7. The rising values of Bi_T expands the temperature of fluid so that $\theta(\eta)$ and the thermal boundary layer thickness becomes heightened due to increment in Bi_T. Similar behavior is observed in fig. 8 also. Whenever M takes larger values, the temperature profile is increased. This is due to the transverse effect of magnetic field on electrically conducting fluid is the reason for existence of Lorentz's forces. These forces slow down the motion of the fluid and rises the fluid temperature. Therefore, thermal boundary layer is thicker with increased magnetic effect.

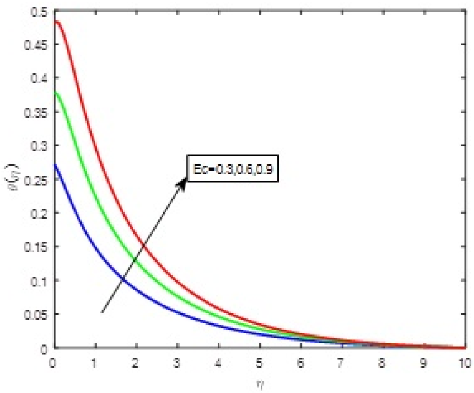

Fig. 5 Consequence of Ec on Temperature

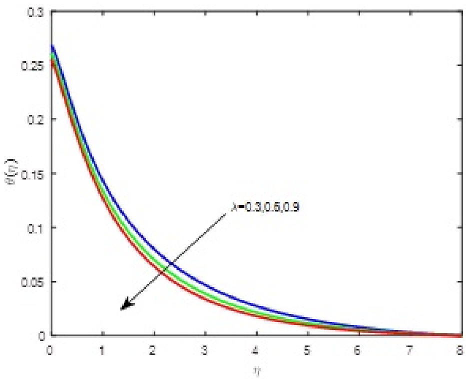

Fig. 6 Consequence of λ on Temperature

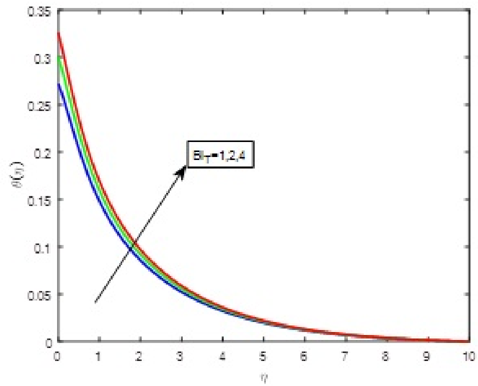

Fig. 7 Consequence of Bi_T on temperature

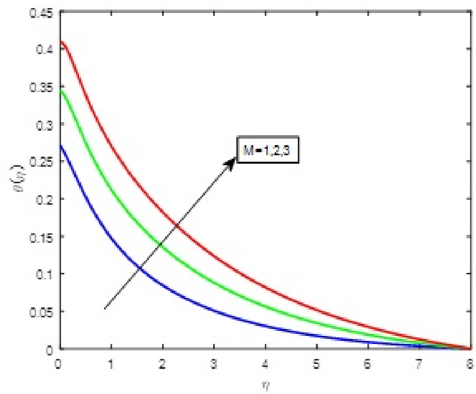

Fig. 8 Consequence of M on temperature

The variations in concentration profile $\phi(\eta)$ are observed from the figures 9 to 11. Fig. 9 depicts the influence of chemical reaction parameter (K_r) on the concentration field. There is some reduction in $\phi(\eta)$ with the enhanced values of K_r. The consequence of concentration biot number (Bi_C) on concentration field is observed in fig. 10. It is clear that the rise in Bi_C creates expansion in concentration field so that concentration curves are heightened. This shows the enhanced effect of Bi_C thicker the concentration boundary layer. From fig. 11 one can notice that the concentration profile $\phi(\eta)$ is seen to be diminished by an increase in Schmidt number (Sc).

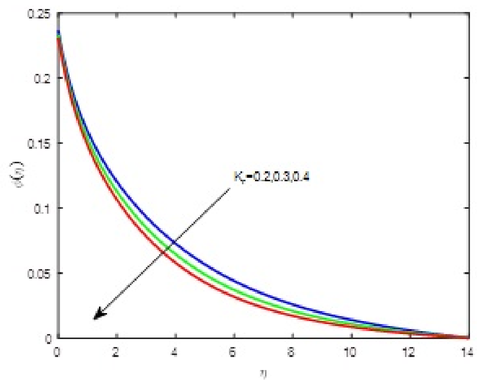

Fig. 9 Consequence of K_r on Concentration

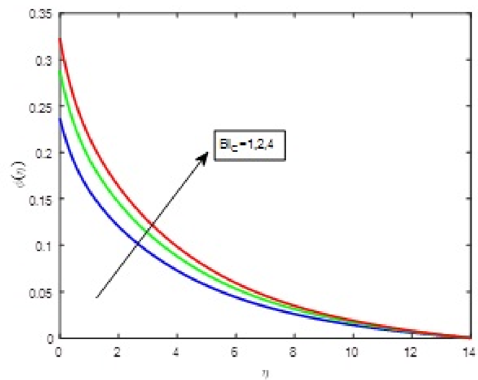

Fig. 10 Consequence of Bi_C on Concentration

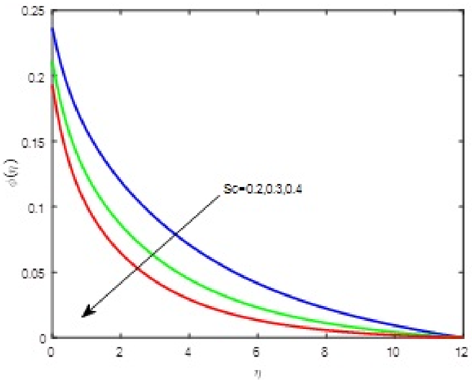

Fig. 11 Consequence of Sc on Concentration

Table-1 shows the values of Nusselt number $'-\theta'(0)'$ for different values of Prandtl number while the remaining parameters taken to be $\Lambda = \lambda = M = Ec = Sc = K_r = 0$ and $a = b = 1$ for comparing them with published results. These results got good agreement with the published work.

Table 1: Comparison of $'-\theta'(0)'$ calculated by Khalili et al. [19] and present study

Pr	**Khalili et al. [19]**	**Present study**
1	0.954955	0.954953
2	1.471421	1.471422
3	1.869044	1.869042
5	2.500109	2.500107

In Table-2, the outcomes of non-dimensional parameters versus friction coefficient, Nusselt number and Sherwood number are noted. It was noticed that when the effect of magnetic field is increased, the friction coefficient and both transfer rates are lowered. Enhancement in both thermal and concentration biot numbers, gives a rise in skin friction and also in both transfer rates. The rise in non-Newtonian fluid parameter (Williamson parameter) gives some decrement in both transfer rates but skin friction is slightly increased. Friction coefficient and heat transfer rate are lowered whenever the Schmidt number is increased but Sherwood number is slightly increased. The rise in Eckert number gives the decrement in heat transfer while some increment is noticed in friction coefficient and Sherwood number. The enhancement in mixed convection parameter implies the considerable hike in skin friction and also in both transfer rates. Also skin friction and rate of heat transfer are diminished but Sherwood number is slightly increased whenever chemical reaction rate is increased.

Table-2 : Computational values for skin friction coefficient, transfer rates (heat and mass)

Λ	Sc	Ec	Bi_T	Bi_C	M	K_r	λ	C_{fx}	Nu_x	Sh_x
0								-1.861781	0.104390	0.138925
0.15								-1.760780	0.097122	0.137264
0.3								-1.617801	0.083376	0.134800
	0.2							-1.759631	0.095813	0.131285
	0.3							-1.760782	0.095516	0.156397
	0.4							-1.761597	0.095318	0.174695
		0.3						-1.759696	0.095866	0.131757
		0.6						-1.740965	-0.010069	0.132935
		0.9						-1.722882	-0.112899	0.133999
			1.0					-1.759696	0.095866	0.131757
			2.0					-1.756116	0.133942	0.131943
			4.0					-1.753005	0.167193	0.132102
				1.0				-1.759602	0.095795	0.131054
				2.0				-1.758040	0.096070	0.159660
				4.0				-1.756973	0.096256	0.179265
					1.0			-1.759857	0.096023	0.132761
					2.0			-2.162934	0.023548	0.123315
					3.0			-2.485720	-0.040927	0.116798
						0.2		-1.759602	0.095795	0.131054
						0.3		-1.759773	0.095732	0.134129
						0.4		-1.759922	0.095679	0.136852
							0.3	-1.738430	0.099916	0.138201
							0.6	-1.674638	0.107024	0.140643
							0.9	-1.614473	0.112778	0.142703

5. Conclusion

Numerical investigation corresponding to the behaviors of heat as well as mass transfers from the exponentially vertical stretching surface of a steady two dimensional Williamson fluid flow along with the influence of magnetic field, viscous dissipation and admissible convective boundary conditions has been carried out. From this study, we conclude that

- Increased Williamson parameter and magnetic effect lowers the fluid velocity.
- Enhanced magnetic effect and thermal biot number elevates the fluid temperature.
- Concentration boundary layer is observed to be thicker by concentration biot number and thinner by chemical reaction parameter.
- Fluid temperature is a decreasing function of mixed convection and increased function of magnetic impact.
- It was also noticed that when the Schmidt number is increased the concentration profile is reduced.
- Skin friction and both transfer rates (heat and mass) lowered by magnetic effect and increased by both biot numbers.

6. Acknowledgments

The corresponding author conveys his sincere thanks to the authorities of his working institute for their encouragement and providing computational facilities to do research.

References

[1] Al-Odat, M. Q., Damseh, R. A., Al-Azab, T. A., Thermal Boundary layer on an exponentially stretching continuous surface in the presence of magnetic field effect, Int. J. of Applied Mechanics and Engineering, Vol.11, No.1 (2006), 289-299.

[2] Anantha Kumar, K., Sugunamma, V., Sandeep, N., Effect of thermal radiation on MHD Casson fluid flow over an exponentially stretching curved sheet, J Therm Anal Calorim 140 (2020), 2377–2385.

[3] Anantha Kumar, K., Sugunamma, V., Sandeep, N., Influence of viscous dissipation on MHD flow of micropolar fluid over a slendering stretching surface with modified heat flux model, J Therm Anal Calorim 139 (2020), 3661–3674. https://doi.org/10.1007/s10973-019-08694-8

[4] Anantha Kumar, K., Sugunamma, V., Sandeep, N., Impact of Non-linear Radiation on MHD Non-aligned Stagnation Point Flow of Micropolar Fluid Over a Convective Surface, Journal of Non-Equilibrium Thermodynamics, Volume 43, Issue 4, 327–345, DOI: https://doi.org/10.1515/jnet-2018-0022

[5] Anantha Kumar K., Ramana Reddy J. V., Sugunamma, V., Sandeep, N., Magnetohydrodynamic Cattaneo-Christov flow past a cone and a wedge with variable heat source/sink, Alexandria Engineering Journal, 57 (2018), 435-443.

[6] Anuar Ishak, Roslinda Nazar, Ioan Pop, Boundary layer flow and heat transfer over an unsteady stretching vertical surface, Meccanica, 44 (2009), 369-375.

[7] Bilal, S., Khalil Ur Rehman, Malik, M.Y., Numerical investigation of thermally stratified Williamson fluid flow over a a cylindrical surface via Keller box method, Results in Physics, 7 (2017), 690-696.

[8] Elbahbeshy, E. M. A., Heat transfer over an exponentially stretching continuous surface with suction, Arch. Mech. 53(6), (2001), 643-651.

[9] Ganesh Kumar, K., Rudraswamy, N. G., Gireesha, B. J., Manjunatha, S., Non linear thermal radiation effect on Williamson fluid with particle-liquid suspension past a stretching surface, Results in Physics, 7 (2017), 3196-3202.

[10] Jayachandra Babu, M., Sandeep, N., MHD non-Newtonian fluid flow over a slandering stretching sheet in the presence of corss-diffusion effects, Alexandria Engineering Journal, 55 (2016), 2193-2201.

[11] Kempannagari A K, Buruju R R, Naramgari S, Vangala S., Effect of Joule heating on MHD non-Newtonian fluid flow past an exponentially stretching curved surface, Heat Transfer, (2020), 1–18. https:// doi.org/ 10.1002/ htj. 21789

[12] Kempannagari Anantha Kumar, Vangala Sugunamma, Naramgari Sandeep, Thermophoresis and Brownian motion effects on MHD Micropolar nanofluid

flow past a stretching surface with non-uniform heat source/sink, Computational Thermal Sciences: An International Journal, Vol.12, No.1 (2020), 55-77.

[13] Kumar, K. A., Sugunamma, V., Sandeep, N., Simultaneous solutions for first order and second order slips on micropolar fluid flow across a convective surface in the presence of Lorentz force and variable heat source/sink, Sci Rep 9, 14706 (2019). https://doi.org/10.1038/s41598-019-51242-5

[14] Kumar K A, Sugunamma V, Sandeep N., A non – Fourier heat flux model for magnetohydrodynamic micropolar liquid flow across a coagulated sheet, Heat Transfer—Asian Res, (2019), 1-25. https://doi.org/10.1002/htj.21518

[15] Kumar, K. A., Sandeep, N., Sugunamma, V., Numerical investigation ofMHD nonlinear radiative oblique flow of micropolar liquid past a stretching sheet with porous medium, Spec. Topics Rev. Porous Media Int. J., 10(6) (2019), 585–605.

[16] Liu, I-Chung, Wang, Hung-Hsun, Peng, Yih-Ferng, Flow and Heat transfer for three-dimensional flow over an exponentially stretching surface, Chemical Engineering Communications, 200 (2013), 253-268.

[17] Magyari, E., Keller, B., Heat and mass transfer in the boundary layers on an exponentially stretching continuous surface, J. Phys. D, Appl. Phys. 32 (1999), 577-585.

[18] Mukhopadhyay, S., Layek, G.C., Effects of thermal radiation and variable fluid viscosity on free convective flow and heat transfer past a porous stretching surface, International journal of Heat and Mass Transfer, 51 (2008), 2167-2178.

[19] Noran Nur Wahida Khalili, Abdul Aziz Samson, Ahmad Sukri Abdul Aziz, Zaileha Md Ali, Chemical reaction and radiation effects on MHD flow past an exponentially stretching sheet with heat sink, IOP Conf. Series: Journal of Physics: Conf. Series, 890 (2017), 012025.

[20] Pal, Dulal, Mixed convection heat transfer in the boundary layers on an exponentially stretching surface with magnetic field, Applied Mathematics and Computation, 217 (2010), 2356-2369.

[21] Parmar, Amit, Unsteady Convective Boundary Layer Flow for MHD Williamson Fluid Over an Inclined Porous Stretching Sheet with Non-Linear Radiation and Heat Source, Int. J. Appl. Comput. Math, 3, (July 2017), 859-881.

[22] Partha, M. K., Murthy, P. V. S. N., Rajasekhar, G. P., Consequence of viscous dissipation on the mixed convection heat transfer from an exponentially stretching surface, Heat Mass Transfer, 41 (2005), 360-366.

[23] Siti Suzilliana Putri Mohamed Isa, Norihan Md. Arifin, Roslinda Nazar, Norfifah Bachok, Fadzilah Md. Ali, The effect of convective boundary condition on MHD mixed convetion boundary layer flow over an exponentially stretching vertical sheet, IOP Conf. Series: Journal of Physics: Conf. Series, 949 (2017), 012016.

[24] Sohail Naeem, Shehla Zaheer, Tiegang Fang, Effects of thermal radiation on the boundary layer flow of a Jeffrey fluid over an exponentially stretching surface, Numer Algor, 57 (2011), 187-205.

[25] Srinivasa Babu, K. S., Parandhama, A., Bhuvana Vijaya, R., MHD Mixed Convection at a Stretching Vertical Sheet with Convective Boundary Condition, International Journal of Recent Technology and Engineering (IJRTE), Vol. 8, No.1S3, (June 2019), 162-165.

[26] Tlili, I., Mustafa, M. T., Kumar, K. A., Effect of asymmetrical heat rise/fall on the film flow of magnetohydrodynamic hybrid ferrofluid, Sci Rep 10 (2020), 6677. https://doi.org/10.1038/s41598-020-63708-y

[27] Tsai, R., Huang, K. H., Huang, J. S., Flow and heat transfer over an unsteady stretching surface with non-uniform heat source, International Communications in Heat and Mass Transfer, 35 (2008), 1340-1343.

[28] Williamson, R. V., The flow of pseudoplastic materials, Ind. Eng. Chem. 21, 11 (1929), 1108-1111.